CdZnTe Semiconductor Parallel Strip Frisch Grid Radiation Detectors

D.S McGregor[1], Z. He[1], H.A. Seifert[1], R.A. Rojeski[2], and D.K. Wehe[1]
[1]Department of Nuclear Engineering and Radiological Sciences, University of Michigan, MI 48109-2100
[2]Etec Systems, Inc., 26460 Corporate Ave., Hayward, CA 94545

Abstract

CdZnTe wide band gap compound semiconducting material offers promise as a room temperature operated gamma ray spectrometer. Position-dependent free charge carrier losses during transport can prevent efficient charge carrier extraction from semiconductor detectors and severely reduce energy resolution. Hole trapping losses in CdZnTe radiation detectors are far worse than electron trapping losses and resolution degradation in CdZnTe detectors results primarily from severe hole trapping during transport. Coplanar radiation detectors improve energy resolution by sensing the induced charge primarily from the motion of electrons. Demonstrated is an alternative approach to single free charge carrier sensing, in which a parallel strip Frisch grid is fabricated on either side of a parallelepiped block. The detectors are three terminal devices, but require only one preamplifier for the output signal. The prototype devices demonstrate a considerable increase in energy resolution when operated in the true Frisch grid mode rather than the planar mode, with a demonstrated room temperature energy resolution for 662 keV gamma rays of 5.91% at FWHM for a 10mm x 2mm x 10mm device. Presently, high surface leakage currents prevent large voltages from being applied to the devices, which ultimately reduces their maximum achievable energy resolution. Further improvements are expected with the realization of reduced surface leakage currents.

I. INTRODUCTION

The material requirements for a room temperature operated high resolution semiconductor gamma ray spectrometer include large free charge carrier mobilities (μ), or alternatively, high achievable free charge carrier velocities (v), long mean free drift times (τ^*), a relatively large energy band gap (E_g) generally between 1.4 eV to 2.5 eV, high representative values of atomic number (Z), and availability in large volumes. Presently, no semiconductor has all of the listed ideal material properties desired for the "perfect" room temperature operated semiconductor radiation spectrometer, although many have a considerable fraction of the required properties (see references 1 and 2). Some wide band gap compound semiconductors that offer promise as room temperature operated gamma ray spectrometers include GaAs, HgI_2, PbI_2, CdTe, and CdZnTe. One difficult problem to resolve with these materials is gamma ray energy resolution degradation from charge carrier trapping losses [3,4].

The general planar detector design that is used for compound semiconductor radiation detectors consists of a block of material with contacts fabricated on either side of the block. Spectroscopic measurements of gamma radiation interactions require that both electrons and holes be extracted efficiently from a conventional planar detector [4], hence the device dimensions are usually tailored to reduce trapping effects from the most effected charge carrier (usually holes). Generally, compound semiconductors have notable differences between the mobilities and mean free drift times of the electrons and holes. For instance, CdZnTe material has reported mobility values of 120 cm^2/V-s for holes and 1350 cm^2/V-s for electrons. Additionally, the reported mean free drift times are $2x10^{-7}$ s for holes and 10^{-6} s for electrons. Hence, the effect of trapping losses is much more pronounced on holes than on electrons, and the device dimensions would have to be designed to compensate for the problem.

A similar situation is experienced with gas filled ion chambers, in which electron-ion pairs are produced by gamma ray interactions in the gas. The electron mobilities are much higher than the positive ion mobilities, hence the extraction times of the electrons are considerably less than the extraction times of the ions. For typically used integration times, the measured pulse amplitude becomes dependent on the initial gamma ray interaction location in the ion chamber [5]. As a result, wide variations in pulse amplitude are possible. The problem was significantly reduced by Frisch with the incorporation of a grid in the ion chamber near the anode [6]. The measured pulses from the detector corresponded to only the movement of mobile charges in the region between the grid and the anode, hence ion movement in the bulk of the device no longer effected the signal output.

The Frisch grid concept has been demonstrated with semiconductor detectors using a coplanar design [7-12]. The devices work well, but unlike the true Frisch grid, they generally require more than one output signal or a circuit capable of discerning the different grid signals. Presented in the following work are results from true Frisch grid semiconductor detectors. The detectors have parallel strip Frisch grids across their bulk and require only one output each to any standard charge sensitive preamplifier circuit.

II. THEORETICAL CONSIDERATIONS AND DETECTOR DESIGN

A simple planar semiconductor detector is operated by applying a bias voltage across the bulk of the material. Ionizing radiation excites electron-hole pairs that are drifted apart by the device electric field. Electrons are drifted towards the anode and holes are drifted towards the cathode. An induced charge is produced at the terminals of the device by the moving free charge carriers, and the induced charge can be measured by an externally connected circuit. Shockley [13] and Ramo [14] derived the dependence of the induced current and induced charge produced by point charges moving between electrodes, which was later shown

0018-9499/98$10.00

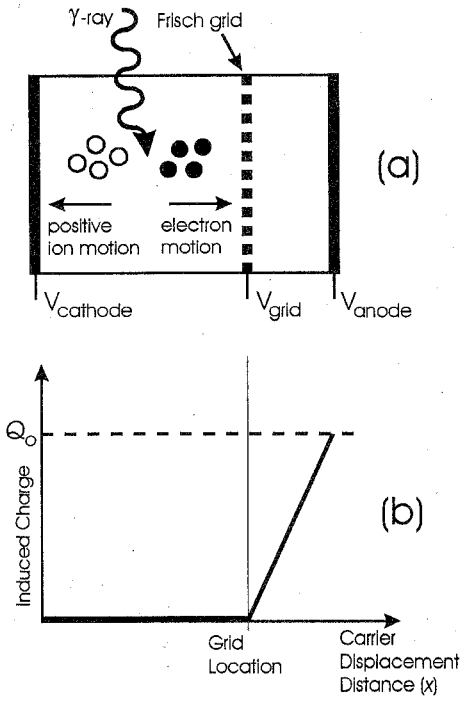

Figure 1. The basic configuration for the Frisch grid gas detector. (a) The gas detector volume is separated into an interaction region and a measurement region. Electron charge carriers are drifted towards the anode by an applied bias. (b) The induced charge that appears at the anode is zero until the electrons pass through the grid. After passing through the grid, a charge is induced proportional to the distance traveled by the charge carriers between the grid and the anode.

to apply to semiconductor detectors as well [15-17]. The Shockley-Ramo theorem shows that the induced charge appearing at the terminals of a planar device from moving point charges is proportional to the distance displaced by the moving point charges, regardless of the presence of space charge. Hence, the change in induced charge Q^* can be represented by

$$\Delta Q^* = Q_o \frac{|\Delta x_e| + |\Delta x_h|}{W_D} \quad , \tag{1}$$

where Q_o is the initial charge excited by the interacting gamma ray, W_D is the detector length, Δx is the distance traveled by the electrons or holes, and the e and h subscripts refer to electrons or holes, respectively. With trapping, the total induced charge from a single gamma ray event in a planar semiconductor detector can be represented by

$$Q^* = Q_o\{\rho_e(1 - \exp[(x_i - W_D)/\rho_e W_D]) + \rho_h(1 - \exp[-x_i/\rho_h W_D])\} \quad , \tag{2}$$

where x_i represents the interaction location in the detector as measured from the cathode and ρ is the carrier extraction factor represented by

$$\rho_{e,h} = \frac{v_{e,h}\,\tau^*_{e,h}}{W_D} \quad , \tag{3}$$

where v is the charge carrier velocity and τ^* is the carrier mean free drift time. From equations 2 and 3, it becomes clear that the induced charge (Q^*) will be dependent on the location of the gamma ray interaction. Small values of ρ for either holes or electrons will cause large deviations in Q^* across the detector width [4]. The induced charge deviation can be greatly reduced if a detector is designed such that the carrier with the longer mean free drift time and highest mobility contributes to all or most of the induced charge.

A Frisch grid gas ion chamber is designed to measure the induced charge primarily from electrons, and the general configuration and operation of a Frisch grid ion chamber is shown in Fig. 1. A gamma ray interaction occurring in the main volume of the detector excites electron-ion pairs. An externally applied electric field drifts the carriers in opposite directions, in which the electrons drift through the grid and into the measurement region of the device. From the Shockley-Ramo theorem, the induced charge produced at the anode results from charge carriers moving between the grid and the anode and not from charge motion between the cathode and the grid. As a result, the detector is primarily sensitive to only the electron charge carriers.

A simple semiconductor Frisch grid detector can be built using the design shown in Fig. 2. As shown, a semiconductor block is cut and polished with metal electrodes fabricated at the ends. These electrodes serve as the anode and cathode. Parallel metal contacts are fabricated on opposite faces of the device, which serve to act as the Frisch grid. The region between the cathode and the parallel Frisch grid is the *interaction region*, the region underneath the parallel grid is the *pervious region*, and the region between the parallel grid

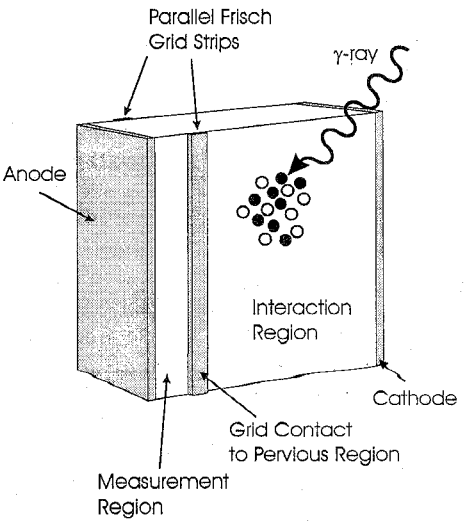

Figure 2. Prototype semiconductor parallel strip Frisch grid design, showing the anode, cathode, and parallel grid configuration. Charge carriers are excited in the interaction region and the electrons are drifted through the parallel strip Frisch grid to the measurement region by an applied electric field.

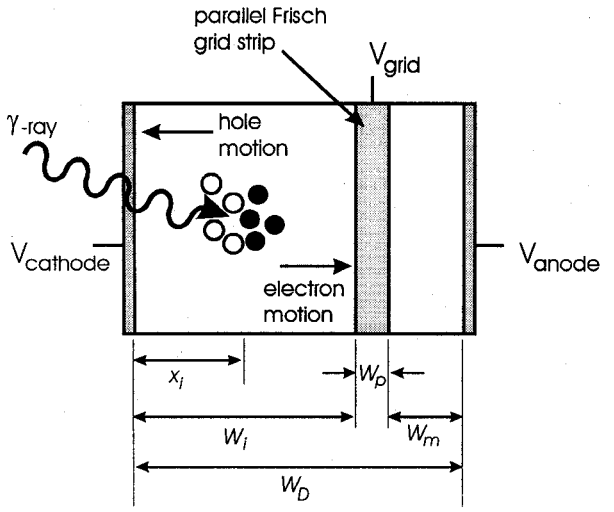

Figure 3. The interaction region is much larger than the measurement region. As a result, *most* of the measured induced charge appears from electrons drifted from the interaction region into the measurement region and *not* from electron-hole pairs excited in the measurement region.

and the anode is the *measurement region*. The device is a *three terminal* device, with the electrodes biased such that electrons are drifted from the interaction region, through the pervious region between the parallel grid, and into the device measurement region.

The different regions and their designations are again shown in Fig. 3. A gamma ray event occurring in the interaction region will excite electron-hole pairs. Electrons are swept from the interaction region towards the parallel grid, however some trapping will occur as the electrons drift across the interaction region and the measurement region. Including the effect of trapping, the measured induced charge from electrons excited in the interaction region by a gamma ray event at a distance x_i from the cathode will be

$$Q^* = K(x,y)Q_o\ \rho_{em}\left(1-\exp\left[\frac{-1}{\rho_{em}}\right]\right)\exp\left[\frac{x_i-\frac{W_p}{2}-W_i}{v_e\tau_e^*}\right], \quad (4)$$

where $K(x,y)$ is a correction factor for deviations in the weighting potential across the device and

$$\rho_{em,hm} = \frac{v_{e,h}\,\tau_{e,h}^*}{\left(\frac{W_p}{2}+W_m\right)}, \quad (5)$$

where the symbols are shown in Fig. 3. It is assumed that the induced charge on the anode begins to increase primarily as the electrons transit across the middle of the pervious region. For gamma ray interactions that occur directly in the measurement region, the induced charge will now be dependent on both electron and hole motion within the measurement region. Including the effects of electron and hole trapping, the induced charge from gamma ray events occurring in the measurement region is

$$Q^* = Q_oK(x,y)\rho_{em}\left(1-\exp\left[\frac{(x_i-W_D)}{\rho_{em}\left(\frac{W_p}{2}+W_m\right)}\right]\right) + Q_oK(x,y)\rho_{hm}\left(1-\exp\left[\frac{(W_D-x_i-W_m-\frac{W_p}{2})}{\rho_{hm}\left(\frac{W_p}{2}+W_m\right)}\right]\right). \quad (6)$$

The device is designed such that the measurement region is considerably smaller than the interaction region. Assuming fairly uniform irradiation of the device (for instance, from the detector side), the fraction of events occurring in the interaction region can be approximated by

$$F_i \approx \frac{W_i+\frac{W_p}{2}}{W_D} = \frac{2W_i+W_p}{2(W_i+W_p+W_m)}. \quad (7)$$

Two CdZnTe parallel strip Frisch grid detectors were designed and tested [18]. Detector 1 has dimensions of 5mm x 2mm x 5mm. The parallel strips were 0.5 mm wide and were fabricated onto the 5mm x 5mm faces at a distance of 1 mm back from the anode. Detector 2 has dimensions of 10mm x 2mm x 10mm. The parallel strips were 1 mm wide and were fabricated onto the 10mm x 10mm faces at a distance of 2 mm back from the anode.

The calculated weighting potentials [17,19] of the two parallel strip Frisch grid CdZnTe detectors are shown in Figs. 4 and 5. The weighting potential shows the normalized change of induced charge on the anode as a function of the free charge carrier location. Figures 4 and 5 show that most of the induced charge will appear as charge carriers move between the anode and the parallel grid, indicating that the parallel grid design should operate as a true Frisch grid detector. Weighting potential deviation in the interaction region is more apparent for the smaller device (5mm x 2mm x 5mm) than the larger device (10mm x 2mm x 10mm). However, in both cases the amount of deviation is 5% or less of the overall weighting potential.

III. Detector Operation and Experimental Results

Detector 1 (5mm x 2mm x 5mm) was operated with the anode grounded and the cathode held at –400 volts. Operating voltages above 400 volts caused unacceptably high surface leakage currents. The detector was tested with the parallel Frisch grid off (floating) and biased at –80 volts.

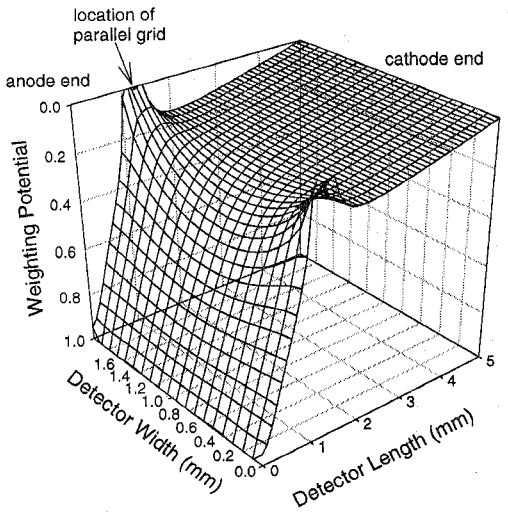

Figure 4. The calculated weighting potential of the 5mm x 2mm x 5mm CdZnTe parallel strip Frisch grid radiation spectrometer. The calculation shows that most of the induced charge will occur from charge carriers transiting the measurement region between the anode and the parallel grid.

Figure 6 shows the calculated operating potential distribution in the device with the grid on. The device was uniformly irradiated from the side by 662 keV gamma rays from a calibrated ^{137}Cs source. Figure 7 shows room temperature spectra from the device with the grid off and on. With the grid off, no discernable full energy peak is apparent. However, a gamma ray peak becomes clearly obvious when the parallel grid is on. The measured energy resolution of the

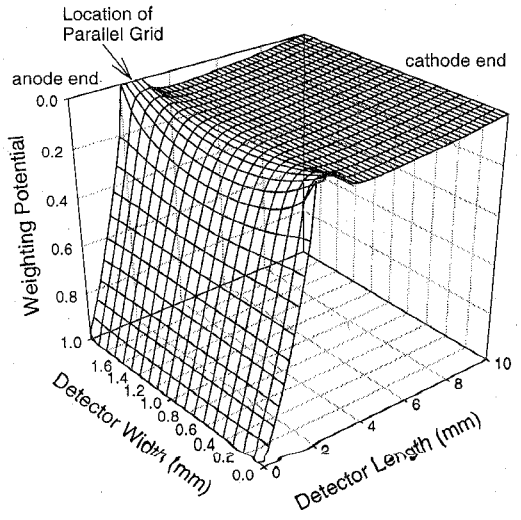

Figure 5. The calculated weighting potential of the 10mm x 2mm x 10mm CdZnTe parallel strip Frisch grid radiation spectrometer. The calculation shows that most of the induced charge will occur from charge carriers transiting the measurement region between the anode and the parallel grid. Less deviation is apparent across the interaction region as compared to the smaller detector.

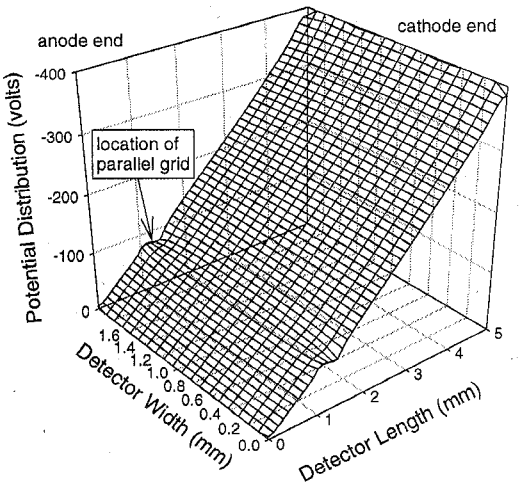

Figure 6. The calculated potential distribution in the 5mm x 2mm x 5mm CdZnTe parallel strip Frisch grid spectrometer with the grid biased at –80 volts.

662 keV peak is 6.2% at FWHM.

To demonstrate that the parallel strip Frisch grid was functioning properly, a 2 cm thick lead attenuator was placed between the ^{137}Cs gamma ray source and the detector such that gamma rays entered only into the interaction region of the device. As a result, all pulses observed from the detector under test were from charge carrier motion originating from the interaction region of the detector. The arrangement used for the test is shown in Fig. 8. Shown in Fig. 9 are spectra taken with the parallel strip Frisch grid off (floating) and turned on (–80 volts). No full energy peak is apparent when the parallel grid is off, however a full energy peak with 4.5% energy resolution at FWHM becomes obvious when the grid is on. It becomes clear that the device is operating as a true single carrier sensitive semiconductor Frisch grid.

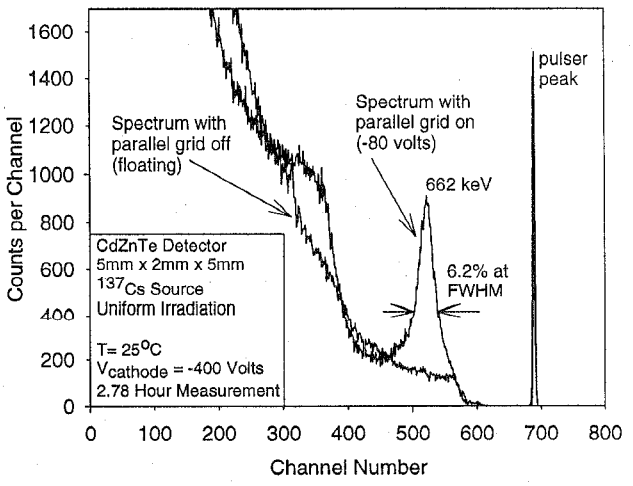

Figure 7. Room temperature spectra of 662 keV gamma rays from the 5mm x 2mm x 5mm CdZnTe semiconductor parallel strip Frisch grid detector with the grid off (floating) and on (-80 volts).

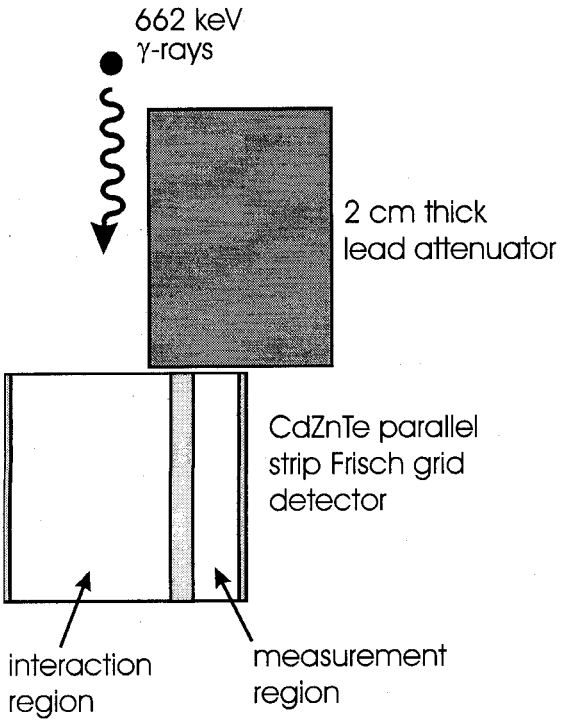

Figure 8. Arrangement used to irradiate only the interaction region of the 5mm x 2mm x 5mm parallel strip Frisch grid detector with 662 keV gamma rays.

Detector 2 (10mm x 2mm x 10mm) was operated with the anode grounded, the cathode biased at –400 volts, and the parallel grid either off (floating) or on (-70 volts). Again, severe surface leakage currents prevented the application of operating voltages above 400 volts across the detector bulk. Figure 10 shows the calculated potential distribution across the device with the grid floating, and Fig. 11 shows the calculated potential distribution across the device with the grid on. Electrons in the device will drift through the parallel

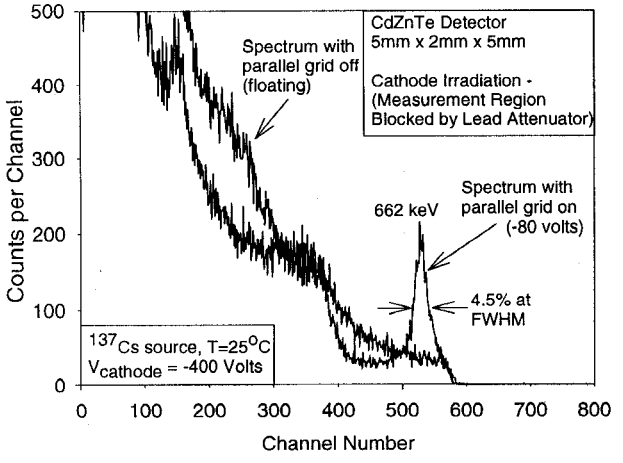

Figure 9. Room temperature spectra of 662 keV gamma rays from the 5mm x 2mm x 5mm CdZnTe semiconductor parallel strip Frisch grid detector with the grid off (floating) and on (-80 volts). The detector has been shielded with a lead attenuator such that gamma rays interacted only in the interaction region.

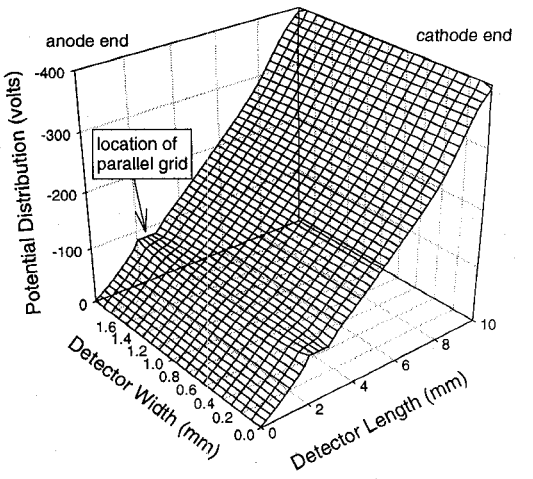

Figure 10. The calculated potential distribution in the 10mm x 2mm x 10mm CdZnTe parallel strip Frisch grid spectrometer with the grid floating.

grid to the anode and holes in the device will drift towards the cathode. Figures 10 and 11 show that there is only a minor difference between the two cases, hence the change in spectra is not due to an enhanced electric field across the measurement region when the grid is turned on.

Figure 12 shows room temperature spectra taken with the 10mm x 2mm x 10mm CdZnTe parallel strip Frisch grid semiconductor spectrometer with the grid off and on. With the grid off, a barely discernable full energy peak is apparent. With the grid on, the 662 keV peak becomes obvious, with a measured energy resolution of 5.91% at FWHM. As indicated from the calculated weighting potentials in Figs. 4 and 5, the induced charge deviation

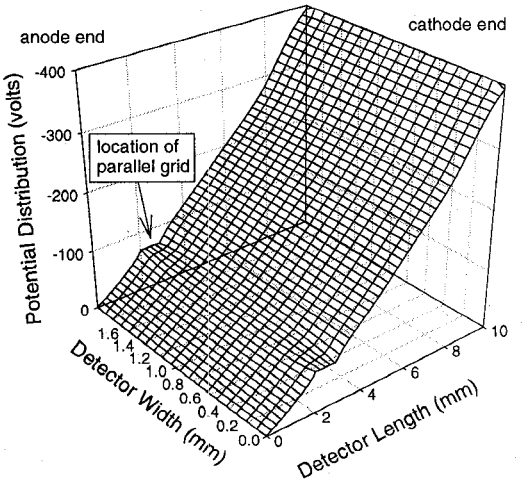

Figure 11. The calculated potential distribution in the 10mm x 2mm x 10mm CdZnTe parallel strip Frisch grid spectrometer with the grid biased at –70 volts.

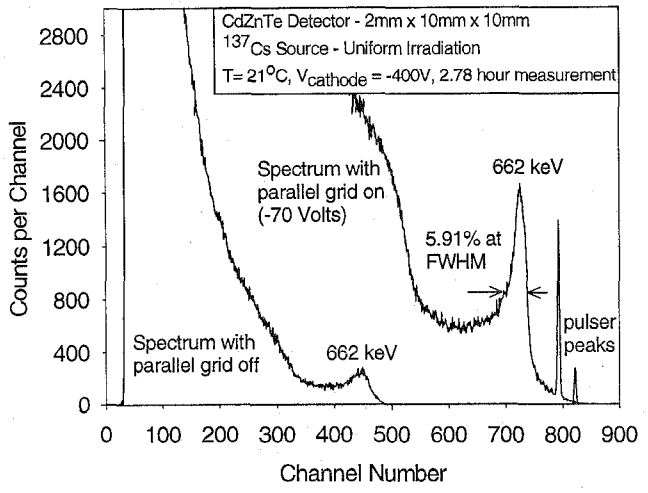

Figure 12. Room temperature spectra of 662 keV gamma rays from the 10mm x 2mm x 10mm CdZnTe semiconductor parallel strip Frisch grid detector with the grid off (floating) and on (-70 volts).

across the interaction region of the 10mm x 2mm x 10mm device should be less than that of the 5mm x 2mm x 5mm device, which may explain why the resolution is better for the large detector. The weighting potentials for the devices are different primarily because the width to length ratio is smaller for the 10mm x 2mm x 10mm detector than the 5mm x 2mm x 5mm detector. As a result, the parallel grids help to flatten the weighting potential in the interaction region more so for the larger detector than the smaller detector. The result indicates that a thicker device (10mm x 4mm x 10mm) would have a similar weighting potential as the 5mm x 2mm x 5mm device.

Also apparent is the fact that the pulse height dramatically increased when the grid was turned on. This observation can be explained as a consequence of the difference in the method by which the induced charge is formed on the anode. When operated with the grid floating, the detector performs as a simple planar detector with 1 cm of material between the anode and the cathode. Equation 2 describes the expected induced charge as a function of the gamma ray interaction depth. Since the carrier extraction factors are much higher for electrons than holes, the largest induced charge pulse will appear from electrons that are excited near the cathode. The low bias voltage of –400 volts produces a relatively low electric field across the device, hence the electron velocity is relatively low, and the electrons will undergo some appreciable trapping before reaching the anode. The resulting maximum pulse height measured by the external circuit is relatively low. When the grid is activated, the largest induced charge pulse is generated by electrons excited in the middle of the pervious region. These electrons have undergone no appreciable trapping before entering the measurement region, and the resulting pulse height corresponding to the induced charge will be much higher (as observed). The observed spectra from the CdZnTe detector with the grid off and on further demonstrates that the detector is operating as a true semiconductor Frisch grid device.

IV. Conclusions

Two CdZnTe semiconductor parallel strip Frisch grid radiation spectrometers have been demonstrated as viable room temperature operated gamma ray spectrometers. The devices operate as true Frisch grid detectors, and demonstrate dramatic improvement when the parallel grids are activated as opposed to the parallel grids being off. Room temperature energy resolution for 662 keV gamma rays is presently 6.2% at FWHM for the smaller device and 5.91% at FWHM for the larger device. Severe surface leakage currents prevent biases greater than 400 volts to be applied across the detectors. The low voltages do not allow the electron charge carriers to gain sufficient velocity to reduce trapping. As a result, the devices do not perform according to their theoretical maximum as calculated from equations 4 and 6. Hence, improved surface passivation and reduction of the surface leakage current is mandatory for better spectroscopic performance. Regardless, the devices performed well under the circumstances, and offer an interesting method to improve energy resolution for compound semiconductor radiation detectors.

V. References

[1] T.E. Schlesinger and R.B. James, Semiconductors for Room Temperature Nuclear Detector Applications, in Semiconductors and Semimetals, Vol. 43, Academic Press: San Diego, 1995.

[2] D.S. McGregor and H. Hermon, "Room Temperature Compound Semiconductor Radiation Detectors," Nucl. Inst. and Meth., Vol. A 395, pp. 101-124, 1997.

[3] R.B. Day, G. Dearnaley, and J.M. Palms, "Noise, Trapping and Energy Resolution in Semiconductor Gamma-Ray Spectrometers," IEEE Trans. Nucl. Sci., Vol. NS-14, pp. 487-491, 1967.

[4] G.F. Knoll and D.S. McGregor, "Fundamentals of Semiconductor Detectors for Ionizing Radiation," Proc. MRS, Vol. 302, pp. 3-17, 1993.

[5] G.F. Knoll, Radiation Detection and Measurement, 2nd. Ed., Wiley: New York, 1989.

[6] O. Frisch, British Atomic Energy Report, BR-49 (1944).

[7] P.N. Luke, "Single-Polarity Charge Sensing in Ionization Detectors using Coplanar Electrodes," Appl. Phys. Lett., Vol. 65, pp. 2884-2886, 1994.

[8] P.N. Luke, "Unipolar Charge Sensing with Coplanar Electrodes – Application to Semiconductor Detectors," IEEE Trans. Nucl. Sci., Vol. NS-42, pp. 207-213, 1995.

[9] Z. He, "Potential Distribution Within Semiconductor Detectors Using Coplanar Electrodes," Nucl. Instr. and Meth., Vol. A 365, pp. 572-575, 1995.

[10] Z. He, G.F. Knoll, D.K. Wehe, R. Rojeski, C.H. Mastrangelo, M. Hammig, C. Barrett, and A. Uritani, "1-D Position Sensitive Single Carrier Semiconductor Detectors," Nucl. Instr. and Meth., Vol. A 380, pp. 228-231, 1996.

[11] Z. He, G.F. Knoll, D.K. Wehe, and J. Miyamoto, "Position-Sensitive Single Carrier CdZnTe Detectors," Nucl. Instr. and Meth., Vol. A 388, pp. 180-185, 1997.

[12] M. Amman and P.N. Luke, "Coplanar-Grid Detector with Single-Electrode Readout," in Hard X-Ray and Gamma-Ray Detector Physics, Optics, and Applications, *R. B. Hoover, F. P. Doty, Eds.*, Proc. SPIE, Vol. 3115, pp. 205-213, 1997.

[13] W. Shockley, "Currents to Conductors Induced by a Moving Point Charge," J. Appl. Phys., Vol. 9, pp. 635-636, 1938.

[14] S. Ramo, "Currents Induced by Electron Motion," Proc. IRE, Vol. 27, pp. 584-585, 1939.

[15] G. Cavelleri, G. Fabri, E. Gatti, and V. Svelto, "On the Induced Charge in Semiconductor Detectors," Nucl. Instr. and Meth., Vol. 21, pp. 177-178, 1963.

[16] M. Martini and G. Ottaviani, "Ramo's Theorem and the Energy Balance Equations in Evaluating the Current Pulse from Semiconductor Detectors," Nucl. Instr. and Meth., Vol. 67, pp. 177-178, 1969.

[17] G. Cavelleri, G. Fabri, E. Gatti, and V. Svelto, "Extension of Ramo's Theorem as Applied to Induced Charge in Semiconductor Detectors," Nucl. Instr. and Meth., Vol. 92, pp. 137-140, 1971.

[18] The devices were custom fabricated to our specifications and delivered by eV Products, 375 Saxonburg Blvd., Saxonburg, PA 16056.

[19] V. Radeka, "Low Noise Techniques in Detectors," Ann. Rev. Nucl. Part. Sci., Vol. 38, pp. 217-277, 1988.